Journal of Organometallic Chemistry, 336 (1987) 29–43
Elsevier Sequoia S.A., Lausanne – Printed in The Netherlands

Borole derivatives

X *. Syntheses of (η^5-borole)metal complexes via borole ammonia adducts. Complexes of the chromium group metals and the crystal and molecular structures of tetracarbonyl [η^5-(1-phenylborole)]chromium and its molybdenum analogue

G.E. Herberich*, B. Hessner, M. Negele

Institut für Anorganische Chemie der Technischen Hochschule Aachen, Professor-Pirlet-Str. 1, D-5100 Aachen (F.R.G.)

J.A.K. Howard

Department of Inorganic Chemistry, The University, Cantock's Close, Bristol BS8 1TS (Great Britain)

(Received May 12th, 1987)

Abstract

The 1*H*-Borole ammonia adducts $C_4H_4BR \cdot NH_3$ (R = Me, Ph) (Ia,b) have been made by ammonia degradation of the (η^5-borole)carbonyliodocobalt complexes $(C_4H_4BR)Co(CO)_2I$ (VIa,b). They are the simplest 1*H*-borole derivatives obtained to date, and have been identified in solution by NMR spectroscopy. Reactions starting from Ia,b have given otherwise inaccessible (η^5-borole)metal complexes such as (η^5-C_4H_4BMe)$Cr(CO)_4$ (II) and (η^5-C_4H_4BPh)$M(CO)_4$ (III: M = Cr, IV: M = Mo, V: M = W). X-ray diffraction studies on III and IV show them to have distorted piano stool structures with bond lengths Cr–B 240.3(2) and Mo–B 253.4(4) pm. Site exchange processes within the $M(CO)_4$ groups are fast on the ^{13}C NMR time scale even at 155 K.

1*H*-Boroles are 4π-electron systems with a small HOMO/LUMO separation. As a consequence, simple, i.e. *C*-unsubstituted 1*H*-boroles, are unknown, and only a few sterically protected 1*H*-boroles are known [2–4]. Because of this, synthetic procedures for the preparation of (η^5-borole)metal complexes usually avoid free 1*H*-boroles as ligand sources although in the case of pentaphenylborole this route has been used with some success [3]. The most satisfactory route to (η^5-borole)metal complexes involves the reaction of dihydroboroles (2-borolenes and 3-borolenes) [5]

* For part IX see Ref. 1.

0022-328X/87/$03.50

with suitable transition metal compounds which, in many cases, results in dehydrogenating complex formation [6]; suitable substrates are the carbonyls of Mn [7], Fe [7], Ru [1], Os [1], and Co [7], various complexes of Ru [1], Rh [1], and Os [1], including Cramer's complex $[Rh(\eta\text{-}C_2H_4)_2Cl]_2$ [1,8], and Wilkinson's catalyst $RhCl(PPh_3)_3$ [1]. Alternative routes are known, but are rather limited in scope [9–12].

In this paper we report on a novel synthetic method involving generation of the borole ammonia adducts Ia, b, and subsequent use of these adducts to form new complexes. As examples we chose the (η^5-borole)tetracarbonylmetal compounds II–V, which are not accessible from borolenes and chromium group metal hexacarbonyls by dehydrogenating complex formation.

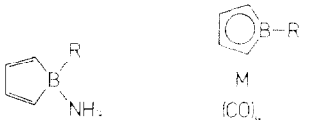

(Ia: R = Me; Ib: R = Ph)

(II: M = Cr, R = Me; III: M = Cr, R = Ph; IV: M = Mo, R = Ph; V: M = W, R = Ph)

Borole Lewis-base adducts

(η^5-Borole)metal complexes show little tendency to release the organic ligand, but we found that the carbonyliodocobalt complexes VIa,b [13] readily react with ammonia in ether or THF above −30 °C. Details of the ensuing reaction sequence will be described elsewhere, and here we describe only the overall result.

When an excess of gaseous ammonia is introduced into a solution of VIa in THF the colour changes and evolution of CO is observed above −30 °C. At room temperature a deep red solution and an insoluble pink powder, $[Co(NH_3)_6]I_2$, are obtained. The ^{11}B NMR spectrum of the solution shows a narrow signal ($\delta(^{11}B)$ −5.5 ppm, line width 80 Hz) for Ia and a broad signal ($\delta(^{11}B)$ +25 ppm) for several labile, not fully identified (η^5-borole)carbonylcobalt species, which slowly decompose to give the known dinuclear complex VIIa [13]. Similarly, the phenyl compound VIb gives the adduct Ib ($\delta(^{11}B)$ −4.6 ppm, line width 110 Hz). The only known borole derivative with a similar C-unsubstituted structure is the cyanoborate $[CoCp_2]^+ \cdot$ VIIIb [8].

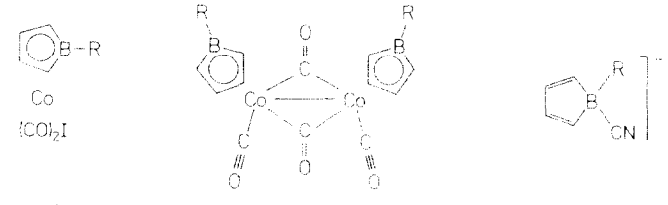

(VI) (VII) (VIII)

(a: R = Me
b: R = Ph)

The adducts Ia,b decompose upon removal of the solvent in vacuo. In solution, they are stabilized by dissolved ammonia and are sufficiently stable for spectroscopic study. Decomposition is fast above 60 °C, especially in the case of Ia, and is accompanied by the appearance of new ^{11}B signals ($\delta(^{11}B)$ +27 and +34 ppm), which may indicate ring opening and formation of borazines (with typical $\delta(^{11}B)$ values of 30–34 ppm [14]).

The NMR data for the new compounds are listed in Tables 1 and 2. For the purpose of comparison, data for the salts IXa,b ≡ $[NMe_3Ph]^+ \cdot$ VIIIa,b are included. Adduct formation by organoboranes has long been known to be accompanied by a large high-field shift of the ^{11}B resonance [17]. In addition, line broadening caused by the quadrupolar relaxation mechanism is much reduced in these adducts [18]. The ^{11}B signals ascribed to Ia,b nicely fit this general pattern.

In the ^{13}C NMR spectra the resonances of the carbon atoms adjacent to the boron appear as very broad signals at room temperature. Below −50 °C effective decoupling of the quadrupolar $^{10}B(^{11}B)$ nuclei [19] is observed, thus allowing precise location of these signals for Ia,b and IXa,b (Table 2). The carbon atoms in the β position to the boron resonate at somewhat higher field than those in the α position. In contrast, vinylboranes [20] (including 2-borolenes [5]), phenylboranes [19], and, as it appears from the available data [4] probably also boroles, show the β carbon resonances at very low field. This effect is attributed to an orbital interaction between the empty p_z orbital of the boron and the ethylenic double bond, and consequently disappears upon adduct formation.

The ^1H NMR signals from Ia,b are broad, possibly owing to the presence of traces of paramagnetic material. The olefinic protons are found in the normal spectral region (cf. cyclopentadiene (liquid): $\delta(^1H)$ 6.28, 6.43 ppm [21]), but the expected AA′BB′ pattern cannot be resolved. Two NH_3 proton signals are found, a singlet for dissolved ammonia ($\delta(^1H)$ 0.39 ppm) and a broad signal for the boron-bonded NH_3 in Ia,b at much lower field. Obviously, NH_3-exchange is slow with respect to the NMR time scale at room temperature.

NMR experiments with Ib in THF also demonstrate exchange at room temperature of the stabilizing Lewis base. Addition of a few drops of pyridine and subsequent removal of the ammonia in a gentle vacuum gives the pyridine adduct X ($\delta(^{11}B)$ +2.4 ppm) which is also formed by degradation of VIb with pyridine in THF. Trimethylphosphine slowly produces the adduct XI ($\delta(^{11}B)$ −12.1 ppm, $^1J(^{31}P-^{11}B) \approx 40$ Hz) which may be compared with $Me_3B \cdot PMe_3$ ($\delta(^{11}B)$ −12.3 ppm [22]) and $(CH_2{=}CH)_3B \cdot PMe_3$ ($\delta(^{11}B)$ −17.5 ppm, $^1J(^{31}P-^{11}B)$ 47 Hz [20]). Furthermore, addition of powdered potassium cyanide to Ib in acetonitrile followed by stirring at room temperature for 36 h brings about quantitative formation of what, on the basis of its ^{11}B NMR spectrum ($\delta(^{11}B)$ −15.1 ppm), is judged to be the anion VIIIb (−15.3 ppm [8]).

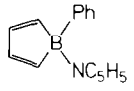

(X)

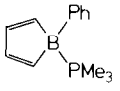

(XI)

(Continued on p. 35)

Table 1

^{1}H NMR and ^{11}B NMR data

Compound	^{1}H NMR [a]			^{11}B NMR [b]	Solvent
	Borole ring		Other groups		
	H(2)/H(5)	H(3)/H(4)			
Ia	6.1m (4H) [c]		−0.25s (Me), 5.1s(br) (NH_3)	−5.5	THF-d_8
Ib	6.3m (4H) [c]		7.0–7.3m (5H) (Ph), 4.7s(br) (NH_3)	−4.6	THF-d_8
II	3.26m (2H)	5.37m (2H)	0.59s(Me)	21.8	CD_2Cl_2
III	3.80m (2H)	5.49m (2H)	7.70m ($2H_o$), 7.36m($2H_m$, H_p)	22.8	CD_2Cl_2
IV	3.98m (2H)	5.57m (2H)	7.62m ($2H_o$), 7.27m ($2H_m$, H_p)	24.9	CD_2Cl_2
V	4.13m (2H)	5.59m (2H)	7.66m ($2H_o$), 7.33m ($2H_m$, H_p)	23.3	CD_2Cl_2
IXa	6.26br (4H)		−3.6s (Me), 7.89m ($2H_o$), 7.57m ($2H_m$, H_p), 3.61s (3Me)	−19.0	THF-d_8
IXb	6.40br (4H)		7.81–7.31m (7H), 6.88m ($2H_m$, H_p), 3.42s (3Me)	−15.6	THF-d_8

[a] $\delta(^{1}H)$ (ppm) relative to internal TMS, 80 MHz. [b] $\delta(^{11}B)$ (ppm) relative to external $BF_3 \cdot OEt_2$, 32.08 MHz. [c] Signals not resolved.

Table 2

^{13}C NMR data [a]

Compound	Borole ring		Other groups	Solvent
	C(2)/C(5)	C(3)/C(4)		
Ia	149d [b] (140)	135.5 (151, 8)	3.0q (Me) [b] (115)	THF-d_8
Ib	150d [b] (145)	138.8 (150, 8)	152 (C_i) [b], 132.9dm (C_o), 127.2dm (C_m), (155,6) (155,6) 125dm (C_p) (156)	THF-d_8
II	85.0d [b] (155)	94.5ddd (174, 11, 7)	−3.1q (Me) [b], 231.6s (CO) (118)	CD_2Cl_2
III	83.1d [b] (158.5)	95.6ddd (172, 10, 6)	135.7dm (C_o), 135.6s (C_i) [b], 129.4dm (C_p) (159.5, 7, 6) (160, 8, 7) 128.3dm (C_m), 232.5s (CO) (158.5, 5, 2)	CD_2Cl_2
IV	83.8d [b] (155)	94.0ddd (171.5, 11, 6)	135.6dm (C_o), 135.2s (C_i) [b], 129.5dm (C_p) (156, 8.5, 5) (156, 8, 7) 128.3dm (C_m), 221.4s (CO) (159.5, 7, 3.5)	CD_2Cl_2
V	80.3d [b] (157.5)	89.6ddd (173.5, 10.5, 7)	135.4dm (C_o), 134.2s (C_i) [b], 129.4dm (C_p), (157.5, 10, 6) (159.5, 7.5) 128.2dm (C_m), 211.0s (CO) [c] (157.5, 6.5, 3)	CD_2Cl_2
VIIIa [d]	154.8dq (139)	135.9dd (150, 9)	4.1q (Me), 143.5q (CN) [f] (112)	THF-d_8
VIIIb [d]	153.3d (138)	137.6ddd (152.5, 14, 9)	152.5s (C_i), 134.3dm (C_o), 127.3dm (C_m), (156) (156) 124.2dm (C_p), 141.0s (CN) (158)	THF-d_8

[a] $\delta(^{13}C)$ (ppm) relative to internal TMS, 67.88 MHz; $J(^{13}C-^{1}H)$ (Hz) in parentheses. [b] Observed at 203 K. [c] $J(^{183}W-^{13}C)$ 130 Hz. [d] As $[NMe_3Ph]^+$ salt; cation signals (cf. [15]) not listed. [e] $^{1}J(^{13}C-^{11}B)$ 56 Hz. [f] $^{1}J(^{13}C-^{11}B)$ 52 Hz; cf. $[BH_3(CN)]^-$: $\delta(^{13}C)$ 146.5 ppm, $^{1}J(^{13}C-^{11}B)$ 53 Hz [16].

Table 3

Preparative data and elemental analyses

Complex	Formula	Mol. weight (g/mol)	MS [a]	Analyses (Found (calc) (%))		Colour	M.p./Dec. (°C)
				C	H		
II	$C_9H_7BCrO_4$	241.96	242	44.56 (44.68)	3.06 (2.92)	yellow	21/160
III	$C_{14}H_9BCrO_4$	304.03	304	55.18 (55.31)	3.06 (2.98)	lemon-yellow	75/180
IV	$C_{14}H_9BMoO_4$	347.97	350	48.41 (48.32)	2.53 (2.61)	dark yellow	74/230
V	$C_{14}H_9BO_4W$	435.88	436	38.43 (38.58)	2.06 (2.08)	orange-yellow	86/280

[a] Parent ion based on most frequent isotopic combination.

Complexes from borole ammonia adducts

Thermal reaction of Ib (prepared from VIb and ammonia in THF as described above) with an excess of the tetrahydrofuran derivatives $M(CO)_5(THF)$ (M = Cr, Mo, W) (ratio 1/3) at 60 °C affords the [η^5-(1-phenylborole)]tetracarbonylmetal complexes III–V, together with the carbonyl compounds $M(CO)_6$, $M(CO)_5(NH_3)$ and the ubiquitous dinuclear cobalt species VIIb (eq. 1). Addition of a $M(CO)_3$ group to the phenyl substituent is an unimportant side reaction, which in the chromium system gives traces of the dinuclear complex XII. The synthesis of the methyl compound II is analogous, but somewhat demanding experimentally owing to the volatility, low melting point, and greater sensitivity of this complex towards light. Preparative and analytical data for the new complexes II–V are listed in Table 3.

$$\underset{\text{(Ib)}}{L \cdot NH_3} + 3\ M(CO)_5(THF) \rightarrow M(CO)_6 + M(CO)_5(NH_3) + \underset{\text{(III–V)}}{LM(CO)_4} \qquad (1)$$

(L = C_4H_4BPh; III: M = Cr; IV: M = Mo; V: M = W)

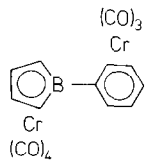

(XII)

The NMR spectra of the new complexes (Tables 1 and 2) show the well established patterns for the *C*-unsubstituted borole ligand with η^5-bonding to the metal. The IR spectra show four ν(CO) bands (Table 4). The number of bands observed excludes a near C_{4v} arrangement of the $M(CO)_4$ group and also a C_{2v} arrangement with two nearly collinear CO groups. As the disposition of the carbonyl groups has been the subject of several theoretical studies [23–26], it seemed worthwhile to undertake an X-ray diffraction study on some of these complexes (see below).

The ^{13}C NMR spectra show only one signal for the CO groups, even at 155 K, thus indicating a low barrier to site exchange processes within the $M(CO)_4$ group. Calculations predict very low barriers to internal rotation for cyclobutadiene complexes such as (η^4-C_4H_4)$Cr(CO)_4$ [23] and for $CpV(CO)_4$ [24]. On the other

Table 4

ν(CO) frequencies (cm^{-1}) [a]

Complex	
II	2052, 1994, 1978, 1961
III	2053, 2002, 1978, 1961
IV	2066, 2005, 1986, 1953
V	2073, 2009, 1977, 1953

[a] In hexane solution.

hand, complexes of open conjugated dienes, such as the butadiene compound $(\eta^4\text{-}C_4H_6)Cr(CO)_4$, are predicted to possess sizeable barriers [26] and, in fact, give temperature dependent ^{13}C carbonyl signals, typically between 180–220 K [27]. We conclude that the more delocalized bonding of a borole as compared to a conjugated diene ligand is responsible for the observed lowering of the barrier.

X-Ray diffraction results

The structure of complex III is illustrated in Figs. 1 and 2, which also show the atom-numbering scheme. The same atom-numbering scheme is used for the structurally very similar molybdenum analogue IV. Details of the structure determinations of III and of IV are given in Table 5. The structures were solved and refined using the SHELX 76 (for III), SHELXTL (for IV) [28] and SDP (for III) [29] program systems, with atomic scattering factors and corrections for anomalous dispersion taken from Ref. 30. The atomic coordinates are given in Table 6, and further structural data in Tables 7 and 8. List of thermal parameters and structure factors are available from the authors.

The structures of III and IV consist of a monofacially bound 1-phenylborole ligand and a tetracarbonylmetal fragment. The crystal structures of the related complexes $(\eta^5\text{-}C_4H_4BPh)Fe(CO)_3$ (XIII) [7], $\mu\text{-}(\eta^5\text{-}C_4H_4BMe)[Co(\eta^5\text{-}C_4H_4BMe)]_2$ [13], $RhCl(\eta^5\text{-}C_4H_4BPh)(PPh_3)_2$ [1], and $RuHCl(\eta^5\text{-}C_4H_4BPh)(PPh_3)_2$ [1] have been described previously.

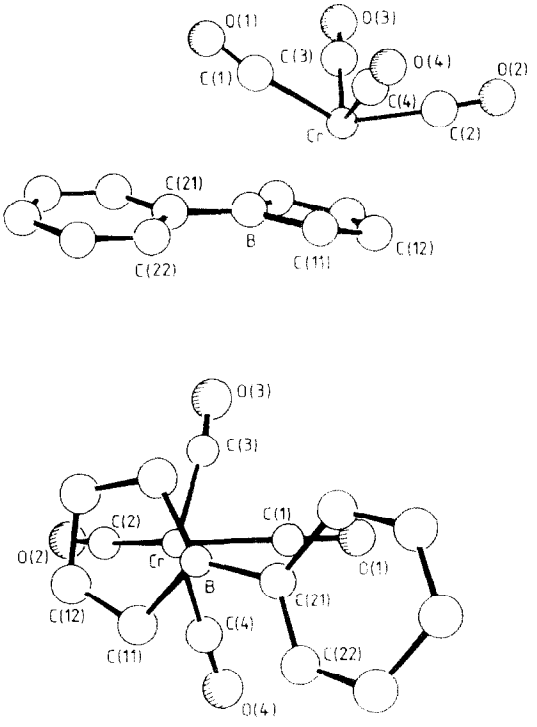

Fig. 1. The molecular structure of III.

Table 5

Crystallographic data, data collection parameters, and refinement parameters

	III	IV
Formula	$C_{14}H_9BCrO_4$	$C_{14}H_9BMoO_4$
Formula weight	304.03	347.97
Space group	$P\bar{1}$ (no. 2)	$P2_1/c$ (no. 14)
a (pm)	657.3(3)	1018.3(7)
b (pm)	962.5(6)	639.2(3)
c (pm)	1095.8(6)	2351.4(19)
α (°)	73.75(4)	
β (°)	82.91(4)	112.18(5)
γ (°)	78.72(5)	
V (nm^3)	0.651(1)	1.417(2)
Z	2	4
d_c (g cm^{-3})	1.551	1.631
Crystal size (nm^3)	$0.4\times0.25\times0.15$ [a]	$0.2\times0.3\times0.6$ [a]
μ (Mo-K_α) (cm^{-1}) [b]	8.8	9.09
Diffractometer	CAD4 (Enraf–Nonius)	P3m (Nicolet)
Radiation, λ (pm)	Mo-K_α, 71.073	Mo-K_α, 71.073
Monochromator	graphite	graphite
Temperature (K)	213	291
Scan mode (θ range (°))	ω–2θ (1–30)	ω–2θ (1.4–25)
No. of unique reflcns [c]	3682	2029
No. of params refined	190	190
R [d]	0.033	0.027
R_w [e]	0.044	0.030
w^{-1}	$\sigma^2(F)+gF^2$ ($g=0.0005$)	$\sigma^2(F)+gF^2$ ($g=0.0003$)

[a] The crystals were sealed under dry dinitrogen in Lindemann capillaries. No significant decay was observed during irradiation. [b] An empirical absorption correction on the basis of azimuthal scans was applied. [c] $I \geq 3\sigma(I)$. [d] $R = \Sigma\|F_o| - |F_c\|/\Sigma|F_o|$. [e] $R_w = [\Sigma w(|F_o| - |F_c|)^2/\Sigma w|F_o|^2]^{1/2}$.

The overall geometry of the borole ligand conforms to the general pattern established previously [1,7,13]. The intra-ring C–C bond lengths for III (140.9/142.1/140.6 pm) indicate that metal-to-ligand back bonding is less important than in the iron complex XIII (with 142.6/141.7/143.5 pm). This effect is even more pronounced for IV (139.7/144.2/139.4 pm). These observations are consistent with the general concept that d^6 $M(CO)_4$ fragments show predominant acceptor character while the opposite holds for d^8 $M(CO)_3$ fragments [23]. The variation of the intra-ring B–C bond lengths (154.0 to 154.9 pm for III and IV, 152.4 to 154.9 pm for all known structures) are of little significance on a 3σ level. The borole rings are folded along the line C(11)–C(14), with comparatively large bending angles of 6.8° for III and 6.2° for IV.

The $M(CO)_4$ fragment can be approximately described by means of two *trans* angles α and β, spanned by the two pairs of *trans* oriented CO groups (cf. Fig. 2). Experimental values are α 115.6 and β 142.6° for III, and α 103.5 and β 151.3° for IV.

The structure of the $M(CO)_4$ fragment is strongly dependent on the nature of the ligand to which it is bonded [23–26]. In the case of weak metal-to-ligand back bonding, the structure should be similar to that of a 1,3-diene complex. Chromium

(Continued on p. 40)

Table 6

Atom coordinates for III and IV [a]

Atom	III (M = Cr)			IV (M = Mo)		
	x	y	z	x	y	z
M	0.25974(4)	0.14681(3)	0.19580(2)	0.10774(2)	0.23778(3)	0.14427(1)
C(1)	0.3431(3)	0.1738(2)	0.3468(2)	0.0096(3)	0.0338(5)	0.1432(2)
C(2)	0.2072(3)	0.0018(2)	0.1235(2)	−0.0321(3)	0.3248(5)	0.1834(1)
C(3)	0.5131(3)	0.0166(2)	0.2109(2)	−0.0312(3)	0.3950(5)	0.0729(2)
C(4)	0.0393(3)	0.0827(2)	0.3105(2)	0.1529(3)	0.0968(6)	0.0752(2)
O(1)	0.3963(2)	0.1771(2)	0.4403(1)	0.1629(2)	0.0120(5)	0.0349(1)
O(2)	0.1830(3)	−0.0901(2)	0.0836(2)	−0.1139(3)	0.3660(4)	0.2031(1)
O(3)	0.6678(2)	−0.0609(2)	0.2150(2)	−0.1083(3)	0.4874(5)	0.0327(1)
O(4)	−0.1005(3)	0.0503(2)	0.3776(2)	−0.0440(3)	−0.1878(4)	0.1454(2)
C(11)	0.0433(3)	0.3603(2)	0.1344(2)	0.3362(3)	0.1367(5)	0.2130(1)
C(12)	0.1014(4)	0.2929(2)	0.0336(2)	0.2712(4)	0.2652(5)	0.2427(1)
C(13)	0.3199(4)	0.2777(2)	0.0042(2)	0.2494(3)	0.4710(6)	0.2156(2)
C(14)	0.4121(3)	0.3366(2)	0.0832(2)	0.2984(3)	0.4804(5)	0.1678(2)
B	0.2373(3)	0.4060(2)	0.1673(2)	0.3699(3)	0.2695(5)	0.1652(2)
C(21)	0.2465(5)	0.5064(2)	0.2553(2)	0.4649(3)	0.2121(5)	0.1280(1)
C(22)	0.0643(3)	0.5770(2)	0.3071(2)	0.5161(3)	0.0112(5)	0.1276(1)
C(23)	0.0689(4)	0.6696(2)	0.3826(2)	0.6037(2)	−0.0384(6)	0.0966(2)
C(24)	0.2563(4)	0.6940(2)	0.4092(2)	0.6390(3)	0.1162(7)	0.0638(2)
C(25)	0.4391(3)	0.6265(2)	0.3589(2)	0.5902(4)	0.3138(7)	0.0628(2)
C(26)	0.4333(3)	0.5349(2)	0.2826(2)	0.5040(3)	0.3629(6)	0.0943(2)

[a] Hydrogen atoms were incorporated at calculated positions (d(C–H) for III 96, for IV 108 pm). Their isotropic thermal parameters were refined.

Table 7

Bond lengths (pm) and bond angles (°) for III and IV

III				IV			
Cr–C(1)	190.5(2)	Cr–C(1)–O(1)	174.1(2)	Mo–C(1)	205.6(4)	Mo–C(1)–O(1)	172.5(3)
Cr–C(2)	188.9(2)	Cr–C(2)–O(2)	176.6(2)	Mo–C(2)	204.3(4)	Mo–C(2)–O(2)	176.6(3)
Cr–C(3)	187.3(2)	Cr–C(3)–O(3)	177.3(2)	Mo–C(3)	201.0(3)	Mo–C(3)–O(3)	178.7(3)
Cr–C(4)	187.8(2)	Cr–C(4)–O(4)	176.6(2)	Mo–C(4)	199.9(3)	Mo–C(4)–O(4)	176.9(3)
C(1)–O(1)	113.2(2)	C(1)–Cr–C(2)	142.6(1)	C(1)–O(1)	112.9(5)	C(1)–Mo–C(2)	151.3(1)
C(2)–O(2)	113.5(2)	C(1)–Cr–C(3)	80.4(1)	C(2)–O(2)	112.6(5)	C(1)–Mo–C(3)	81.7(1)
C(3)–O(3)	113.5(2)	C(1)–Cr–C(4)	80.7(1)	C(3)–O(3)	113.9(4)	C(1)–Mo–C(4)	82.5(2)
C(4)–O(4)	114.0(2)	C(2)–Cr–C(3)	78.3(1)	C(4)–O(4)	113.6(4)	C(2)–Mo–C(3)	81.4(1)
		C(2)–Cr–C(4)	81.3(1)			C(2)–Mo–C(4)	79.1(1)
		C(3)–Cr–C(4)	115.6(1)			C(3)–Mo–C(4)	103.5(1)
Cr–C(11)	224.0(2)	B–C(11)–C(12)	108.4(2)	Mo–C(11)	236.7(3)	B–C(11)–C(12)	108.6(3)
Cr–C(12)	216.9(2)	C(11)–C(12)–C(13)	110.4(2)	Mo–C(12)	229.1(3)	C(11)–C(12)–C(13)	109.8(3)
Cr–C(13)	215.9(2)	C(12)–C(13)–C(14)	110.3(2)	Mo–C(13)	230.1(3)	C(12)–C(13)–C(14)	110.7(3)
Cr–C(14)	223.9(2)	C(13)–C(14)–B	108.4(2)	Mo–C(14)	238.1(3)	C(13)–C(14)–b	108.2(3)
Cr–B	240.3(2)	C(11)–B–C(14)	102.0(2)	Mo–B	253.4(4)	C(11)–B–C(14)	102.3(3)
B–C(11)	154.0(3)	C(11)–B–C(21)	127.7(2)	B–C(11)	154.7(5)	C(11)–B–C(21)	128.9(3)
C(11)–C(12)	140.9(3)	C(14)–B–C(21)	130.1(2)	C(11)–C(12)	139.7(5)	C(14)–B–C(21)	128.6(3)
C(12)–C(13)	142.1(4)	B–C(21)–C(22)	120.7(2)	C(12)–C(13)	144.2(5)	B–C(21)–C(22)	122.1(3)
C(13)–C(14)	140.6(3)	B–C(21)–C(26)	122.5(2)	C(13)–C(14)	139.4(6)	B–C(21)–C(26)	121.3(3)
C(14)–B	154.9(3)			C(14)–B	154.4(5)		
B–C(21)	155.8(2)			B–C(21)	157.3(6)		
C(21)–C(22)	139.6(2)	C(21)–C(22)–C(23)	121.7(2)	C(21)–C(22)	138.7(4)	C(21)–C(22)–C(23)	122.2(3)
C(22)–C(23)	138.2(3)	C(22)–C(23)–C(24)	120.2(2)	C(22)–C(23)	138.6(5)	C(22)–C(23)–C(24)	119.0(3)
C(23)–C(24)	137.7(3)	C(23)–C(24)–C(25)	119.5(2)	C(23)–C(24)	138.1(6)	C(23)–C(24)–C(25)	120.5(4)
C(24)–C(25)	137.8(3)	C(24)–C(25)–C(26)	119.9(2)	C(24)–C(25)	135.4(6)	C(24)–C(25)–C(26)	120.3(4)
C(25)–C(26)	138.3(3)	C(25)–C(26)–C(21)	121.9(2)	C(25)–C(26)	138.3(6)	C(25)–C(26)–C(21)	121.5(3)
C(26)–C(21)	139.3(3)	C(26)–C(21)–C(22)	116.7(2)	C(26)–C(21)	139.7(5)	C(26)–C(21)–C(22)	116.6(3)

Table 8

Definition of best planes, interplanar angles (°), and further structural data for III and IV

		III	IV
Plane A ≡ [C(11) ··· C(14)]	∠ A,B	6.8	6.6
Plane B ≡ [C(11), B, C(14)]	∠ B,C	13.1	9.0
Plane C ≡ [C(21) ··· C(26)]			
Plane D ≡ [C(1), O(1), C(2), O(2)]	∠ D,E	91.0	88.8
Plane E ≡ [C(3), O(3), C(4), O(4)]			
Distance of B atom from plane A (pm)		11.5	11.2
Distance of metal atom from plane A (pm)		184.1	199.9
Slip distortion (pm) [a]		9.6	10.9
C(1)–B (pm)		257.2	265.5

[a] Defined in plane A; distance between projection of metal atom and projection of geometrical centre of C_4B ring; cf. Ref. 7.

group tetracarbonylmetal complexes of 1,3-dienes are comparatively rare [31]; one of the few relevant structures known, is that of the 2,4-hexadiene complex (η^4-MeCH=CHCH=CHMe)$Cr(CO)_2(PMe_3)_2$with *trans* angles α 100.8(10) and 101.1(8)° (C–Cr–C) and β 151.6(2) and 152.4(2)° (P–Cr–P) [32]. On the other hand, the chromium complex III is, in a broad sense, isoelectronic with $CpV(CO)_4$. Thus, in the case of strong back-bonding, the structure of the $M(CO)_4$ group should approach the tetragonal pyramid found in $CpV(CO)_4$ (structure: Ref. 33, bonding: Ref. 24) and in the closely related (η^6-C_5H_5BMe)$V(CO)_4$ [34] with α and β close to 120°. Comparison of the various *trans* angles again confirms that back-bonding is moderate in III, and further decreases on going from III to IV: that is, with decreasing participation in the bonding of the borole LUMO.

The metal–ligand interaction is characterized by a relatively large Cr–B bond length of 240.3(2) pm for III. Somewhat lower values of 236(1) and 236.0(4) pm have been found for the 1,2-diaza-3,6-dibora-4-cyclohexane complex [η^6-$(EtC)_2(BMe)_2(NH)_2$]$Cr(CO)_4$ [35] and for the 1,3-diaza-2,4-diboretidine complex [η^4-$(BuBNBu^t)_2$]$Cr(CO)_4$ [36] respectively. All Mo–C and the Mo–B bond lengths for IV are larger than the corresponding Cr–C and the Cr–B distances by 12–15 pm. The slip distortions (cf. Table 8) of 9.6 pm for III and of 10.9 pm for IV are larger than in the iron complex XIII (6.9 pm [7]). This observation is again related to the weaker back-bonding in III and the even weaker such bonding in IV. It should also be noted that one carbonyl carbon atom is situated underneath the boron atom, giving rise to a remarkably close contact C(1)–B of only 257.2 pm for III (cf. Table 8).

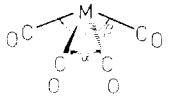

Fig. 2. The *trans* angles α and β of a $M(CO)_4$ fragment of strict or approximate C_{2v} symmetry.

Experimental

Reactions were carried out by standard Schlenk techniques under nitrogen. All solvents were thoroughly dried and deoxygenated.

Ammonia degradation of (η^5-borole)dicarbonyliodocobalt complexes

Dry ammonia (ca. 2 ml, ca. 80 mmol) is added to VIa (1.60 g, 5.0 mmol) [13] in THF or Et_2O (40 ml) at $-78°C$. The mixture is stirred and allowed to warm slowly to room temperature. When gas evolution (CO and NH_3) has ceased, the pink precipitate of $[Co(NH_3)_6]I_2$ is filtered off and washed. The filtrate contains (inter alia) Ia (ca. 2.5 mol, 50%). Ib is obtained analogously from VIb.

Trimethylphenylammonium [1-cyano-1-methylborata-2,4-cyclopentadiene] and trimethylphenylammonium [1-cyano-1-phenylborata-2,4-cyclopentadiene] (IXa,b)

The salts IXa,b are prepared from the triple-decker complexes μ-(η^5-C_4H_4BR)-[Rh(η^5-C_4H_4BR)]$_2$ (R = Me, Ph) by cyanide degradation as described for $[CoCp_2]^+$ · VIIIb [8].

Tetracarbonyl[η^5-(1-methylborole)]chromium (II)

A solution of $Cr(CO)_5(THF)$ in 60 ml THF is prepared from $Cr(CO)_6$ (3.30 g, 15.0 mmol) by exhaustive irradiation with a 150 W high pressure mercury lamp (TQ 150, Original Hanau) and occasional purging with nitrogen of the space above the liquid. A solution of Ia in 40 ml THF, obtained from VIa (1.60 g, 5.0 mmol) and ammonia as described above, is added, and the mixture is kept at 65 °C for 5 h. The solvent is removed under a gentle vacuum. The residue is repeatedly extracted with a total of 150 ml pentane to give a red solution, which is filtered, concentrated to ca. 30 ml and cooled to $-30°C$, to give solid $Cr(CO)_5(NH_3)$ and $Cr(CO)_6$. Chromatography with pentane on alumina (7% H_2O, column 50 cm × 2.0 cm, water-cooled and carefully protected from light) yields four bands: a yellowish forerun containing some $Cr(CO)_6$, a yellow band of II, an orange-red band of VIIa, and a slowly moving yellow band of $Cr(CO)_5(NH_3)$, which can be eluted by adding ether to the eluent. The pentane solution of II is concentrated in a gentle vacuum and the remaining solvent then pumped off at 10^{-5} bar/$-78°C$ to give a crystalline solid. Sublimation (10^{-5} bar) on to a cold finger ($-78°C$) yields 135 mg (0.56 mmol, 11%) II as yellow cristals; m.p. 20–21 °C, dec. > 160 °C, light-sensitive, extremely soluble in all common organic solvents.

Preparation of the 1-phenylborole complexes (III–V)

The complexes III–V are prepared as described for II.

Tetracarbonyl[η^5-(1-phenylborole)]chromium (III). The chromatographic work-up gives one additional band: the lemon-yellow band of II is followed by a second yellow band of XII, which is eluted with pentane/Et_2O (4/1).

III: Crystallisation from hexane at $-30°C$ gives lemon-yellow needles, yield 13.5%, m.p. 74.5–75.5 °C, dec. > 180 °C, light-sensitive in solution.

XII: Yellow solid. MS: *m/e* 440 (M^+). ν(CO) frequencies (hexane): 2050, 1999, 1983, 1977, 1960, 1914sh, 1909 cm^{-1}; for an assignment cf. Table 4. ^1H NMR spectrum ($\delta(^1H)$(ppm), 80 MHz, C_6D_6): 4.65d ($2H_o$), 4.23m ($2H_m$, H_p, H(3), H(4)), 2.76m (H(2), H(5)). $\delta(^{11}B)$: 20 ppm, gg. ext. $BF_3 \cdot OEt_2$.

Tetracarbonyl[η^5-(1-phenylborole)]molybdenum (IV). Crystallisation from hexane at −30 °C gives yellow needles with a slightly greenish tinge, yield 20%, m.p. 73.5–74.5 °C, dec. > 230 °C, somewhat light-sensitive in solution.

Tetracarbonyl[η^5-(1-phenylborole)]tungsten (V). Crystallisation from hexane at −30 °C gives orange-yellow needles, yield 20.5%, m.p. 85–86 °C, dec. > 280 °C.

Acknowledgement

This work was supported by Deutsche Forschungsgemeinschaft and by Fonds der Chemischen Industrie.

References

1 G.E. Herberich, W. Boveleth, B. Hessner, M. Hostalek, D.P.J. Köffer and M. Negele, J. Organomet. Chem., 319 (1987) 311.
2 J.J. Eisch, J.E. Galle and S. Kozima, J. Am. Chem. Soc., 108 (1986) 379; J.J. Eisch, N.K. Hota and S. Kozima, J. Am. Chem. Soc., 91 (1969) 4575.
3 G.E. Herberich, B. Buller, B. Hessner and W. Oschmann, J. Organomet. Chem., 195 (1980) 253.
4 A. Sebald and B. Wrackmeyer, J. Organomet. Chem., 307 (1986) 157; L. Killian and B. Wrackmeyer, J. Organomet. Chem., 148 (1978) 137.
5 G.E. Herberich, W. Boveleth, B. Hessner, M. Hostalek, D.P.J. Köffer, H. Ohst and D. Söhnen, Chem. Ber., 119 (1986) 420.
6 G.E. Herberich, B. Hessner, W. Boveleth, H. Lüthe, R. Saive and L. Zelenka, Angew. Chem. Int. Ed. Engl., 22 (1983) 996; Angew. Chem., Suppl., (1983) 1503.
7 G.E. Herberich, W. Boveleth, B. Hessner, D.P.J. Köffer, M. Negele and R. Saive, J. Organomet. Chem., 308 (1986) 153.
8 G.E. Herberich, W. Büschges, B. Hessner and H. Lüthe, J. Organomet. Chem., 312 (1986) 13.
9 G.E. Herberich, in G. Wilkinson, F.G.A. Stone and E.W. Abel (Eds.), Comprehensive Organometallic Chemistry, Vol. 1, Pergamon Press, Oxford, 1982, p. 381.
10 D.B. Palladino and T.P. Fehlner, Organometallics, 2 (1983) 1692.
11 G.E. Herberich and H. Ohst, Chem. Ber., 118 (1985) 4303.
12 A. Sebald and B. Wrackmeyer, J. Organomet. Chem., 304 (1986) 271.
13 G.E. Herberich, B. Hessner and R. Saive, J. Organomet. Chem., 319 (1987) 9.
14 H. Nöth and B. Wrackmeyer, in P. Diehl, E. Fluck and R. Kosfeld (Eds.), NMR Basic Principles and Progress, Vol. 14, Springer Verlag, Berlin, 1978.
15 H.-O. Kalinowski, S. Berger and S. Braun, ^{13}C-NMR-Spektroskopie, Georg Thieme Verlag, Stuttgart, 1984.
16 L.W. Hall, D.W. Lowman, P.D. Ellis and J.D. Odom, Inorg. Chem., 14 (1975) 580.
17 H. Nöth and H. Vahrenkamp, Chem. Ber., 99 (1966) 1049; H. Nöth and B. Wrackmeyer, Chem. Ber., 107 (1974) 3070.
18 M.J.S. Dewar and R. Jones, J. Am. Chem. Soc., 89 (1967) 2408.
19 J.D. Odom, T.F. Moore, R. Goetze, H. Nöth and B. Wrackmeyer, J. Organomet. Chem., 173 (1979) 15.
20 L.W. Hall, J.D. Odom and P.D. Ellis, J. Am. Chem. Soc., 97 (1975) 4527.
21 M.A. Cooper, D.D. Elleman, C.D. Pearce and S.L. Manatt, J. Chem. Phys., 53 (1970) 2343.
22 J.P. Tuchagues and J.P. Laurent, Bull. Soc. Chim. France, (1971) 4246.
23 M. Elian and R. Hoffmann, Inorg. Chem., 14 (1975) 1058.
24 P. Kubáček, R. Hoffmann and Z. Havlas, Organometallics, 1 (1982) 180.
25 R. Hoffmann, J.M. Howell and A.R. Rossi, J. Am. Chem. Soc., 98 (1976) 2484.
26 T.A. Albright, R. Hoffmann, Y. Tse and T. D'Ottario, J. Am. Chem. Soc., 101 (1979) 3812.
27 M. Kotzian, C.G. Kreiter and S. Özkar, J. Organomet. Chem., 229 (1982) 29.
28 G.M. Sheldrick, Program for Crystal Structure Determination, University of Cambridge, England, 1976; SHELXTL programs for use with the Nicolet X-ray systems, University of Cambridge, 1976, updated Göttingen, 1981.

29 B.A. Frenz, in H. Schenk, R. Olthof-Hazekamp, H. van Koningfeld and G.C. Bassi (Eds.), Computing in Crystallography, Delft University Press, Delft, 1978, p. 64.
30 International Tables for X-Ray Crystallography, Kynoch Press, Birmingham, 1974, Vol. 4.
31 C.G. Kreiter, Adv. Organomet. Chem., 26 (1986) 297.
32 C.G. Kreiter, M. Kotzian, U. Schubert, R. Bau and M.A. Bruck, Z. Naturforsch. B, 39 (1984) 1553.
33 J.B. Wilford, A. Whitla and H.M. Powell, J. Organomet. Chem., 8 (1967) 495.
35 G.E. Herberich, W. Boveleth, B. Hessner, W. Koch, E. Raabe and D. Schmitz, J. Organomet. Chem., 265 (1984) 225.
35 W. Siebert, R. Full, H. Schmidt, J. von Seyerl, M. Halstenberg and G. Huttner, J. Organomet. Chem., 191 (1980) 15.
36 K. Delpy, D. Schmitz and P. Paetzold, Chem. Ber., 116 (1983) 2994.